Identification of the Elemental Composition of Granulated Blast Furnace Slag by FTIR-Spectroscopy and Chemometrics

Authors:

Dmitrii A. Metlenkin, Nikolay V. Kiselev, Yuri T. Platov, Bekzod B. Khaidarov, Timur B. Khaidarov, Evgeniy A. Kolesnikov, Denis V. Kuznetsov, Alexander V. Gorokhovsky, Peter O. Offor, Igor N. Burmistrov

Date Submitted: 2023-02-20

Keywords: chemical composition, chemometrics, infrared spectroscopy, metallurgical slag, PCR, PLS

Abstract:

Blast furnace slag is a key large-tonnage waste product of metallurgical production, which is considered to be a promising alternative material in construction. In order to determine the scope of potential use of slag as a marketable product, it is necessary to study its structure and composition, which is determined by means of modern analytical instrumental methods. This paper analyzes the application of Fourier transform infrared spectroscopy (FTIR) and chemometrics methods to develop calibration models for identifying pelletized slag by elemental composition. In a comparative analysis of FTIR-spectra of slag the characteristic frequencies of absorption bands responsible for the content of calcite, silicates and aluminosilicates in the composition of samples were determined. Multivariate regression methods (principal components regression, partial least squares regression) and data of elemental composition results by EDX method were used to develop calibration models for determining elemental composition of granulated blast furnace slag. Using the developed PLS models with high performance (R2 from 0.91 to 0.96 for different components), the prediction of the elemental composition (Ca, Si, O, Mg) of the test sample was carried out and a low deviation of the prediction in contrast to the EDX reference data was obtained. The use of PLS calibration models for rapid and nondestructive determination of the quantitative content of components of the composition of granulated blast furnace slag has been proposed.

Record Type: Published Article

Submitted To: LAPSE (Living Archive for Process Systems Engineering)

Citation (overall record, always the latest version):	LAPSE:2023.0647
Citation (this specific file, latest version):	LAPSE:2023.0647-1
Citation (this specific file, this version):	LAPSE:2023.0647-1v1

DOI of Published Version: https://doi.org/10.3390/pr10112166

processes

MDPI

Article

Identification of the Elemental Composition of Granulated Blast Furnace Slag by FTIR-Spectroscopy and Chemometrics

Dmitrii A. Metlenkin [1,*], Nikolay V. Kiselev [1,2], Yuri T. Platov [1], Bekzod B. Khaidarov [2], Timur B. Khaidarov [2], Evgeniy A. Kolesnikov [2], Denis V. Kuznetsov [2], Alexander V. Gorokhovsky [2], Peter O. Offor [3] and Igor N. Burmistrov [2,*]

[1] Engineering Center, Plekhanov Russian University of Economics, 115054 Moscow, Russia
[2] Department of Functional Nanosystems and High-Temperature Materials, National University of Science and Technology "MISiS", 119049 Moscow, Russia
[3] Metallurgical and Materials Engineering Department, University of Nigeria, Nsukka 410001, Nigeria
* Correspondence: dametl@mail.ru (D.A.M); glas100@yandex.ru (I.N.B.)

Abstract: Blast furnace slag is a key large-tonnage waste product of metallurgical production, which is considered to be a promising alternative material in construction. In order to determine the scope of potential use of slag as a marketable product, it is necessary to study its structure and composition, which is determined by means of modern analytical instrumental methods. This paper analyzes the application of Fourier transform infrared spectroscopy (FTIR) and chemometrics methods to develop calibration models for identifying pelletized slag by elemental composition. In a comparative analysis of FTIR-spectra of slag the characteristic frequencies of absorption bands responsible for the content of calcite, silicates and aluminosilicates in the composition of samples were determined. Multivariate regression methods (principal components regression, partial least squares regression) and data of elemental composition results by EDX method were used to develop calibration models for determining elemental composition of granulated blast furnace slag. Using the developed PLS models with high performance (R^2 from 0.91 to 0.96 for different components), the prediction of the elemental composition (Ca, Si, O, Mg) of the test sample was carried out and a low deviation of the prediction in contrast to the EDX reference data was obtained. The use of PLS calibration models for rapid and nondestructive determination of the quantitative content of components of the composition of granulated blast furnace slag has been proposed.

Keywords: chemical composition; chemometrics; infrared spectroscopy; metallurgical slag; PCR; PLS

Citation: Metlenkin, D.A.; Kiselev, N.V.; Platov, Y.T.; Khaidarov, B.B.; Khaidarov, T.B.; Kolesnikov, E.A.; Kuznetsov, D.V.; Gorokhovsky, A.V.; Offor, P.O.; Burmistrov, I.N. Identification of the Elemental Composition of Granulated Blast Furnace Slag by FTIR-Spectroscopy and Chemometrics. *Processes* **2022**, *10*, 2166. https://doi.org/10.3390/pr10112166

Academic Editors: Yibing Zuo, Guang Ye and Xiaomei Wan

Received: 28 September 2022
Accepted: 19 October 2022
Published: 22 October 2022

1. Introduction

Metallurgical slag is an inseparable byproduct of ferrous and non-ferrous metal production [1]. Slag formation occurs when the flux material reacts with minerals or with the oxidation products of dissolved elements during mining, smelting, or refining of metals [2]. This produces a melt of complex oxides with a low melting point—slag, which is not mixed with the metal phase and is separated as a byproduct, which is placed in landfills or used for recycling.

Urbanization leads to an increase in construction, increasing cement production and a concomitant increase in carbon dioxide emissions affecting the environment [3]. Metallurgical slags are used as an alternative and promising material used as a primary binder [4,5]. The use of metallurgical slag as a marketable product not only has a positive effect on environmental improvement, but also has economic efficiency [6]. The reduction in total emissions when using metallurgical slag as a construction raw material is due to the involvement of slag in production cycles and is relevant due to the development of decarbonization trends in the industry [7].

The chemical composition, structure and mode of processing into a product affect the technological and operational characteristics of construction materials, including metallurgical slags. The composition of metallurgical slag affects the optimal sphere of its application: high calcium content allows the use of slag in the production of binders for cement, low—in the production of gravel or thermal insulation materials [8,9]. It has been shown [9–11] that metallurgical slag is also used in the production of acid-resistant concrete, slag-glass ceramics, heat-resistant concrete.

Granulated blast furnace slag can also be used for soil stabilization [11]. It was shown [12–15] that the addition of granulated blast furnace slag activates the process of soil chemical stabilization by changing its physical and chemical properties. At the same time, granulated blast furnace slag or its mixtures with fly ash act as compaction agents, binders and water repellents and change the soil behavior [16,17]. The presence of calcium (CaO) in granulated blast furnace slag helps to reduce the setting time and increase the compressive strength of clay soil [18–20]. During the reaction between granulated blast furnace slag and an alkaline activator solution, calcium–aluminate–silicate hydrate (C-A-S-H) is formed, which forms a gel in the geopolymer matrix. Such hydration products as well as the aluminosilicate structure in the granulated blast furnace slag increase the strength properties [21].

In order to determine the optimal application area of metallurgical slag, it is necessary to evaluate elemental and phase composition and morphology. For applications related to slag remelting (incorporation into mineral wool or stone/slag castings), composition plays a key role, while morphology and phase composition are important for applications such as a dispersed additive to mineral binders and cements, and for use as slag slurry and stone.

The study of the composition and structure of metallurgical slag is carried out using various methods, including X-ray diffractometry (XRD), X-ray fluorescence analysis (XRF), electron microscopy and energy-dispersive X-Ray analysis (EDX), optical and spectral methods of analysis [7,22–30]. A brief description of strengths and limitations of these methods are given below.

The application of the method of X-ray diffraction analysis in assessing the composition of slag makes it possible to establish the phase composition of the object [2,7,23,28]. The specified method allows to characterize the slag heterogeneous in chemical composition, to reveal crystalline phases and to estimate the ratio of crystalline and amorphous phases in the slag composition. Among others, there is a method of quantitative nonstandard (evaluation takes place without standard reference samples) of phase composition assessment by the Rietveld method [31]. However, there is no universal procedure of calculation and in each case the approximation of theoretical and experimental X-ray spectra is necessary, which is performed manually. In this connection, the Rietveld method calculation is not highly accurate and reproducible [32].

Another universal method for assessing the structure and composition of solid objects is scanning electron microscopy (SEM). SEM makes it possible to evaluate the structure of an object with considerable resolution, as well as to analyze the elemental composition with high precision. However, this method is expensive to operate and maintain, there is a need to place the sample in a vacuum, the inability to consider non-conductive materials. Moreover, SEM cannot be used for rapid characterization of the composition of the object, as there is no possibility to use a microscope on-line, for example on the production line.

The most common methods for determining elemental composition of slags are X-ray fluorescence analysis (XRF) and energy-dispersive X-ray analysis (EDX) [33]. EDX is a rapid method and allows you to evaluate the composition of certain areas of the sample surface, but the determination of elemental composition is only possible for the upper layers of the sample. In turn, XRF is also a rapid and generally non-destructive method, with fast sample preparation and no daily recalibration of the instrument. However, XRF can face limitations in measuring lighter elements [34].

In turn, spectral techniques make it possible to quickly and accurately determine the composition of not only organic, but also mineral products with minimal sample preparation and in situ. In particular, a number of works [7,25–27] have shown the possibility of characterizing the composition of slag by means of infrared spectroscopy. The application of multivariate analysis methods based on spectral data makes it possible to classify the slags according to the nature of origin, as shown in [22]. Collective of authors [24] demonstrated the use of the procedure of deconvolution of wide absorption bands in the infrared spectrum to find additional groups of components in the composition of slags.

Analysis of the composition of granulated blast furnace slag by deconvolution of FTIR spectra requires additional data processing [7,24], including baseline correction and normalization. In this case, the parameters height, center, and HWHM (half-width at half-maximum) are analyzed after curve fitting. Despite the fact that the deconvolution of FTIR spectra, allows to analyze the composition of the slag, this methodology is not easy to use in industrial applications, because its use in automatic mode seems difficult.

The use of FTIR methods together with the reference analysis for the analysis of metallurgical slag composition has not been used before. In this work, for the first time, we tested an express method of indirect evaluation of metallurgical slag compositions and compared the efficiency of selected methods for slags from four metallurgical works using iron ores from different deposits.

In this connection, the aim of this work is to develop calibration models for determining the elemental composition of blast furnace slag from infrared spectra by multivariate analysis.

2. Materials and Methods

Samples of granulated blast furnace slag, differentiated by the iron ore deposit on the basis of which the blast furnace slag was produced, were selected as objects of research. From these samples a calibration (training) set of samples was made, which was used to build calibration models of elemental composition determination. A sample of metallurgical slag of unknown composition (Russia, JSC «EVRAZ NTMK») was selected as a test sample to check the quality and accuracy of the calibration models. Characteristics and name of the sample of granulated blast furnace slag are presented in Table 1.

Table 1. Characteristics and name of the sample of granulated blast furnace slag.

Iron Ore Deposit on the Basis of Which Granulated Blast Furnace Slag Was Produced, Slag Producer	Set
Kostomukshskoye field, Russia (PAO «Severstal»)	Calibration
Stoilenskoye field, Russia (PAO «NLMK»)	Calibration
Magnitogorskoye field, Russia (PAO «Mechel»)	Calibration
Lisakovskoe field, Kazakhstan (JSC «ArcelorMittal Temirtau»)	Calibration
Fields of the Tagil-Kushvin group, Russia (JSC «EVRAZ NTMK»)	Test

The elemental composition of granulated blast furnace slag samples from calibration and test samples was performed by scanning electron microscopy (SEM) on Tescan Vega3 analyzer (TESCAN, Czech Republic) using SDD-XMAS (Japan) in five repetitions. The data of elemental analysis were taken for powder samples. Samples of granulated slag for analysis were randomly selected from commercially available products. The granulated slag was ground in an agate mortar to a powder fineness allowing more than 95% of the ground fraction to pass freely through a 0.63 mm sieve. Five samples of unsieved powder were taken for analysis, to ensure maximum accuracy and repeatability. The larger fraction can represent separate solid phases with differing composition, so sieving and separation were performed only to assess the degree of grinding, and SEM-EDX analysis was performed for unsieved samples. The averaged elemental composition of EDX spectra of each granulated blast furnace slag sample from calibration samples was used as responses (Y matrix) in development of calibration models for composition determination. SEM and EDX images of metallurgical slags of various origins are presented in Figure 1.

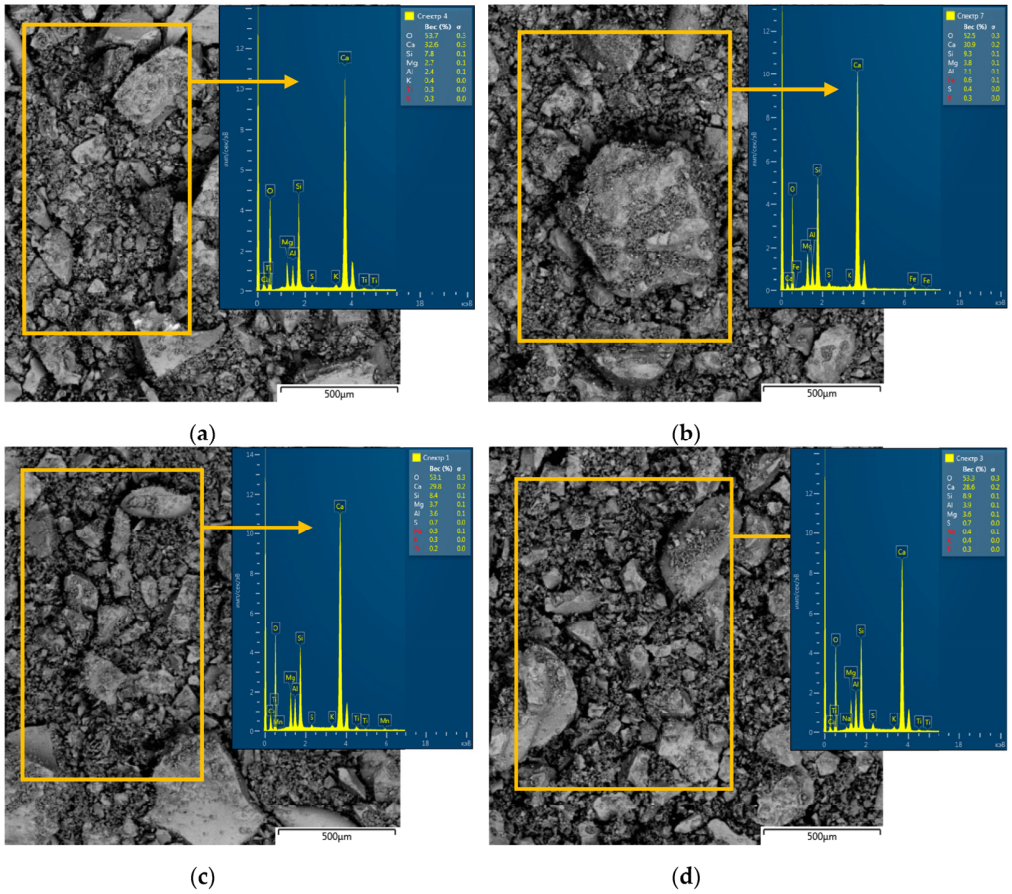

Figure 1. SEM and EDX (a separate samples from a group of averaged) images of metallurgical slags of various origins: (**a**) PAO «Severstal», (**b**) PAO «NLMK», (**c**) PAO «Mechel» and (**d**) JSC «ArcelorMittal Temirtau».

X-ray phase analysis was carried out on an Difray-401k desktop diffractometer (JSC "Scientific Instruments", Russia). The Bragg–Brentano measurement geometry was used, the step-by-step scanning mode (step 0.01 deg) in the measurement range of diffraction angles, 2θ (14–140°). To identify phases in diffraction patterns, the library of the international electronic base of diffraction standards (produced by the International Center for Diffraction Data (ICDD)) was used: PDF-2 (Powder Diffraction File-2) databases in the Crystallographic Search-Match Version 3.1.0.2 software. During the study, the samples were previously pounded in a mortar.

To study the fractional makeup of the milled granulated blast furnace slags from the calibration set the Vibrotechnik VP-30T vibration drive testing sifter and a set of 300×50 mm^2 sieves with brass mesh (mesh size 10.0 mm, 5.0 mm, 1.0 mm, 0.5 mm) were used. The slags were sieved until only uniform particles of similar size were on the sieve. For the subsequent calculation of packed and true density of granulated blast furnace slags from the calibration set standard methods for crude materials were used.

The moisture values of the granulated blast furnace slag samples were obtained using an AXIS AGS-100 moisture analyzer (Poland). The samples were kept at room temperature and humidity for 5 days. The determination of the moisture content was carried out at a temperature of 160. The measurement was stopped when a constant mass was reached.

FTIR spectra were obtained on a Bruker ALPHA spectrometer with ATR (attenuated total reflection) module in the range of 4000–400 cm^{-1} (resolution of 2 cm^{-1}). The slag samples were ground in an agate mortar until a powder of uniform dispersion was obtained to increase the accuracy of the recorded signal and reduce the influence of background noise when measuring FTIR spectra. As a result, we obtained 29 spectra of samples differing

by manufacturer, which were transformed into the data matrix X with the dimension 29 × 1748 (29—number of measurements of spectra of samples, 1748—coefficients of intensity at the wavenumbers of the spectra). To interpret the functional groups of the IR spectra of the components of the composition of the slag, the spectra of each sample were averaged using standard formulas in the MS Excel software package (Microsoft corp., Albuquerque, NM, USA).

To develop calibration models for determining the elemental composition of granular blast furnace slag, we used multidimensional methods: principal components regression (PCR), partial least squares regression (PLS), using the Unscrambler X 10.0.4 software package (Camo Software, Oslo, Norway).

3. Main Results

The analysis of granular blast furnace slags samples was carried out in three stages. At the first stage, analysis of the phase composition of blast furnace slag was carried out by X-ray diffractometry. At the second stage, the interpretation of the absorption bands of the spectra was carried out and the differences between the samples were determined. At the third stage, development of calibration models for the quantitative determination of the components of composition of the samples was carried out based on chemometric algorithms and verification of the models' quality was checked using test-validation on a test sample.

3.1. X-ray Diffractometry

When analyzing the results of X-ray diffractometry revealed a significant amount of silicon oxide in the composition of samples from calibration set, as well as the method of cooling (granulation) give the preconditions for the formation of an amorphous phase (glass phase). Diffractograms of the studied samples from calibration set are shown in Figure 2.

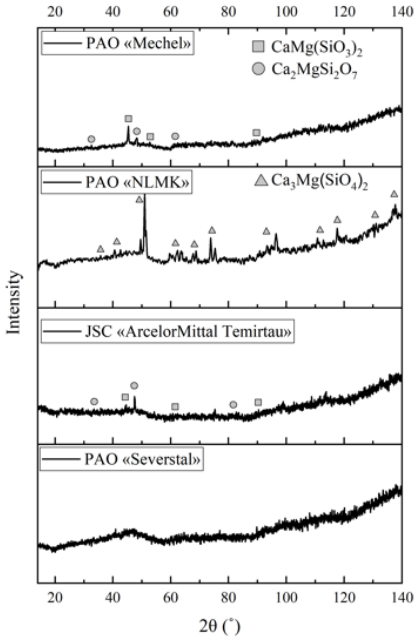

Figure 2. Diffractograms of granulated blast furnace slag from calibration set (PAO Severstal, PAO NLMK, PAO Mechel and JSC ArcelorMittal Temirtau).

The diffractogram of PAO Severstal granulated blast furnace slag does not show pronounced reflexes corresponding to crystalline phases. The sample contains a significant amount of glass phases.

On the diffractogram of PAO NLMK blast-furnace slag sample there are maxima corresponding to mervenite phase ($Ca_3Mg(SiO_4)_2$). This phase has weak hydraulic properties and is in the middle of the series of hydraulic activity of compounds present in slag. In addition to the mervinite phase in the sample there is a significant amount of glass phase.

At the analysis of phase composition of PAO Mechel granulated slag has been established that in addition to the amorphous component, the acermanite ($Ca_2MgSi_2O_7$) and diopside ($CaMgSi_2O_6$) phases are present.

The diffractogram of granulated slag from the JSC ArcelorMittal Temirtau shows reflexes corresponding to acermanite ($Ca_2MgSi_2O_7$) and diopside ($CaMgSi_2O_6$) phases. The presence of a significant amount of glass phase is also noted. Its phase composition is similar to that of PAO Mechel slag.

The phase composition of PAO Mechel and JSC ArcelorMittal Temirtau slag has been found to be similar, and the diffractograms are almost identical. The PAO NLMK slag is highly crystalline, unlike the PAO Severstal glass slag. This information is important for a preliminary assessment of the structure and properties of blast furnace slag, but does not provide comprehensive information on the composition to determine directions for its use.

3.2. Physical and Chemical Properties

Analysis of physical and chemical properties of granulated blast furnace slags is carried out to determine the further direction of using such waste in production of constructional materials and approaches of their technological processing. Table 2 shows moisture and density of granulated blast furnace slags from the calibration set. According to the table, the differences in the parameters Moisture, Packed density and True density in the samples of granulated blast furnace slags from the calibration set are insignificant.

Table 2. Moisture and density of granulated blast furnace slags from the calibration set.

Sample	Moisture, %	Packed Density, kg/m^3	True Density, g/cm^3
PAO Severstal	0.5	1098	2.9
PAO NLMK	1.9	1056	2.9
PAO Mechel	0.3	1140	2.85
JSC ArcelorMittal Temirtau	0.6	1060	2.9

The purpose of sieving was to identify the dominant fraction range for granulated blast furnace slags from the calibration set. Fractional composition of granulated blast furnace slags from the calibration set is shown in Table 3. According to the results of sieving through four sieves, it was found that the fractional composition of slags has a low variability. However, the sample PAO Mechel is characterized by a more homogeneous distribution of particles by size, which in the first approximation allows to recommend this sample for use in the production of slag-alkali binders.

Table 3. Fractional composition of granulated blast furnace slags from the calibration set.

Sample	Hole Size of Test Sieves, mm					Total
	10	5	1	0.5	Less Than 0.5	
PAO Severstal	0	0.9	50.7	38.9	9.5	100
PAO NLMK	0	0.5	50.5	37.4	11.6	100
PAO Mechel	0	1	43.9	42.5	12.5	100
JSC ArcelorMittal Temirtau	0	0.8	58.8	33.8	6.6	100

The elemental composition of the studied samples of granulated blast-furnace slag was studied according to the EDX data taken from different areas and averaged (Table 4). Samples of granulated blast furnace slag from the calibration set have insignificant differences in the content of major elements. Significant presence of O (oxygen) in the composition of

the studied samples is associated with the structure of the material (mineral oxides) and it is consistent with the results of the phase composition established by X-ray diffractometry.

Table 4. Fractional composition of granulated blast furnace slags from the calibration set.

Sample	The Main Elements in the Composition of the Slag					
	O	Ca	Si	Mg	Al	K
PAO Severstal	54.5	32	7.6	2.7	2.4	0.37
PAO NLMK	53.2	30.3	9.3	3.8	2	0.33
PAO Mechel	53.8	31.2	6.9	3.8	2.8	0.3
JSC ArcelorMittal Temirtau	53.3	29.2	8.6	3.6	3.7	0.33

In this study, the analysis of physical and chemical properties of granulated blast furnace slag did not allow to draw conclusions about the differences in the composition of the samples. Thus, establishing a further application of granulated blast furnace slags is not possible. In this regard, the work on the interpretation of FTIR-spectra and the construction of calibration models as presented in the sections below.

3.3. Interpretation of FTIR Spectra

Prior to the development of calibration models, a comparative analysis of the averaged IR spectra of each series of samples of granulated blast furnace slag was carried out (Figure 3). The assignment of spectrum bands to the components of blast furnace slag composition was carried out in accordance with previously published data [7,23–29]. For samples from both the calibration and test sets, the absence of obvious bands and the presence of background noise in the 4000–1600 cm^{-1} region were observed, so a comparative analysis of the spectra was performed in the 1600–400 cm^{-1} region.

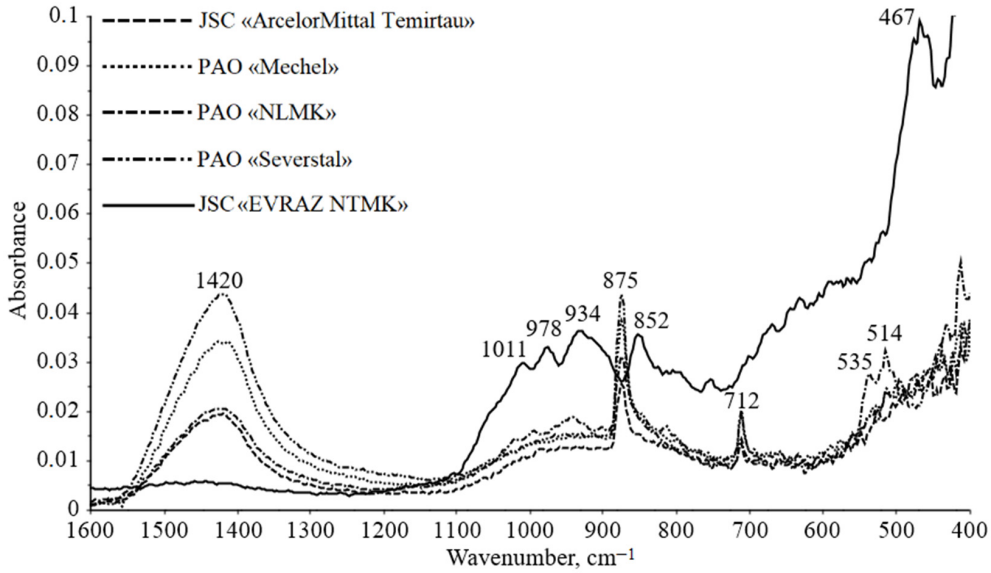

Figure 3. FTIR spectra profile of granulated blast furnace slag samples from calibration (PAO Severstal, PAO NLMK, PAO Mechel and JSC ArcelorMittal Temirtau) and test (JSC EVRAZ NTMK) sets in the range 1600–1200 cm^{-1}.

A comparative analysis of the positions of the maxima and the intensity of the absorption bands of the IR spectra of five samples revealed differences between them, which is associated with differences in the composition of the granulated domain slag (Table 5).

Table 5. Assignment of spectrum bands to components of the chemical composition of granulated blast furnace slag.

Band, cm^{-1}	Band Assignment	Reference
1420	ν_s * CO_3	[22]
1021, 1011 ****	ν_s, ν_{as} ** Si–O	[5,7,25]
992, 978 ****	ν_{as} Si–O–M	[23]
945, 934 ****	ν_{as} Si–O–Si, ν_{as} Si–O–Al	[5,7,25]
875, 852 ****	ν_s CO_3	[22]
712	ν_s CO_3	[23]
535	Δ *** Si–O–Al	[22]
514	δ Si–O–Al	[22,26]
504	δ Si–O (SiO_4)	[24,27]
466	δ Si–O (SiO_2)	[23]

* ν_s—stretching symmetric vibrational modes; ** ν_{as}—stretching asymmetric vibrational modes; *** δ—bending vibrational modes; **** —shifts of absorption bands of the spectrum detected in the test sample.

Among the IR spectra of the samples from the test sample in the 1600–400 cm^{-1} range, the main differences were observed for three absorption bands at 1420, 875 and 712 cm−1, corresponding to vibrations of carbonate groups (CO_3), which constitute calcium carbonates [18]. The test sample lacks an obvious absorption band maximum at 1420 cm^{-1}, there is a shift in the absorption band from 875 cm^{-1} to 852 cm^{-1}, and the absorption band maximum at 712 cm^{-1} enters the broad absorption range of 730–690 cm^{-1}.

The absorption bands in the bands 1100–900 cm^{-1} and 600–400 cm^{-1} (fingerprint region), which are characteristic of the absorption of silicates and aluminosilicates [7,24–30], were also detected. For the PAO "NLMK" sample, absorption bands at 1021, 992 and 945 cm^{-1} are observed, which, according to [23–29], are attributed to Si-O, Si-O-M (M-metal) vibrations. The test sample, unlike the samples from the calibration sample, showed a shift of the Si-O valence vibration band from 1021 cm^{-1} to 1011 cm^{-1}, a shift of the Si-O-M valence vibration band from 992 cm^{-1} to 978 cm^{-1}. According to [26], this shift is due to the silicate content in the slag composition. Indeed, the silicate content in the test sample according to EDX data is 2% higher than the silicate content in the samples from the calibration set.

The PAO "NLMK" sample also exhibited a triplet in the 540–500 cm^{-1} region with absorption maxima at 535, 514, and 504 cm^{-1}, corresponding to the strain vibrations of Si-O-Al and Si-O (SiO_4) [27,28,30]. The presence of three narrow peaks in the spectrum of the PAO "NLMK" sample is probably associated with the formation of silicate crystal structures during melt cooling [35]. The presence of broad absorption bands in these spectral ranges without clear peaks in the remaining samples from the calibration set and, especially, from the test sample testifies to the amorphous state of silicates in these samples, unlike the PAO "NLMK" sample with clear Si-O-Si and Si-O-A vibration absorption bands characteristic of the crystalline phase.

For the test sample, unlike the samples from the calibration set, the Si-O (SiO_2) strain vibration absorption band at 466 cm^{-1} was noted, which also corresponds to a relatively higher silicate content in the test sample.

3.4. Development of Calibration Models for Determining the Elemental Composition of Granulated Blast Furnace Slag

At the stage of preliminary analysis of development of calibration models the following tasks were solved:

- Selection of composition elements as predictors in the development of calibration models (Ca, O, Si, Mg were selected). The selection of predictors was carried out in accordance with [8,9], where the elements of composition influencing the choice of the scope of potential application of the blast furnace slag sample are indicated.
- Selection of the optimal method of multivariate calibration: PCR and PLS (PLS was chosen);

- Building of models with different spectral range (range 1600–400 cm^{-1} was chosen) and number of factors (latent variables) to increase the accuracy of the final models (Table 5);
- Assessment of models' efficiency according to the indices of root-mean-square error of validation and prediction (RMSEV and RMSEP, respectively) and coefficient of determination of validation and prediction (R^2(V) and R^2(P), respectively);
- Verification of calibration models using test-validation (Table 6).

Table 6. Verification of the quality and accuracy of calibration models for determining the components of the composition of granulated blast furnace slag.

Method	Component	Spectral Range, cm^{-1}	Number of Factors	Set	RMSEV/RMSEP	R^2(V)/R^2(P)
PCR	Ca	4000–400	1	Validation Calibration	0.5 0.54	0.76 0.74
PCR	Si	4000–400	2	Validation Calibration	0.55 0.61	0.64 0.58
PCR	O	4000–400	1	Validation Calibration	0.2 0.21	0.84 0.83
PCR	Mg	4000–400	3	Validation Calibration	0.25 0.33	0.73 0.56
PLS	Ca	4000–400	4	Validation Calibration	0.15 0.26	0.97 0.94
PLS	Si	4000–400	4	Validation Calibration	0.12 0.21	0.98 0.95
PLS	O	4000–400	4	Validation Calibration	0.06 0.1	0.98 0.96
PLS	Mg	4000–400	5	Validation Calibration	0.05 0.1	0.99 0.96
PLS	Ca	1600–400	7	Validation Calibration	0.06 0.26	0.99 0.94
PLS	Si	1600–400	5	Validation Calibration	0.1 0.17	0.99 0.96
PLS	O	1600–400	4	Validation Calibration	0.07 0.15	0.97 0.92
PLS	Mg	1600–400	6	Validation Calibration	0.05 0.15	0.99 0.91

The results of the modelling are shown in Table 6.

Based on the results of the modelling, the PLS models in the 1600–400 cm^{-1} range were selected as the most representative ones due to the high R^2 and low RMSE values, affecting the quality and accuracy of the models, respectively. PCR calibration models were not used for test-validation due to low R^2 values. It should be noted that regardless of the choice of predictors, in general the increase in accuracy of all calibration models is associated with the removal of uninformative regions of the IR spectrum from 4000 to 1600 cm^{-1}.

Test-validation of chemometric models for determining the components of the composition of granulated slag was carried out (Table 7). The difference of the results of prediction by the PLS method from the elemental composition data by EDX is ranked in the range of 0.9–6.5% depending on the component being determined. The use of PLS calibration models based on spectral data in the range of 1600–400 cm^{-1} for rapid and nondestructive determination of quantitative content of components of composition of granulated blast furnace slag has been proposed.

Table 7. Assignment of spectrum bands to components of the chemical composition of granulated blast furnace slag.

Component	Content, %wt.		Deviation of PLS from EDX, %
	Prediction by PLS Model	Elemental Composition by EDX	
Ca	18.8 ± 2.6	20.1 ± 1.0	6.5
Si	10.7 ± 2.0	10.6 ± 0.6	0.9
O	50.3 ± 1.6	48.6 ± 1.2	3.5
Mg	5.9 ± 1.5	5.8 ± 0.3	1.7

The comparative analysis of the obtained results with the composition-based recommendations on the basis of works [8,9,36] allows to formulate recommendations on directions of use for granulated blast furnace slag from the test set. JSC «EVRAZ NTMK» granulated blast furnace slag due to its low content of calcium can be recommended for the production of gravel or slag wool. However, these models work well within a homogeneous group of samples, e.g., blast furnace slag. When switching to converter or ferroalloy slags, model modifications will be required.

The application of FTIR spectroscopy to estimate the composition of granulated blast furnace slag is mainly related either to the identification of characteristic spectrum bands [25–27], or to the application of classification methods (PCA, SIMCA) for slag grading [22], or to their search by deconvolution of broad-spectrum bands [7,24]. However, the practical application of the chemometric method to estimate the composition of granulated blast furnace slag is not common enough.

The novelty of our research is the use of FTIR spectroscopy as a simple, rapid and inexpensive way to characterize the composition of blast-furnace slags, primarily by the degree of carbonization of Ca and Mg oxides, which is difficult for traditional X-ray methods [2] but is extremely important for their applications as a raw material for mineral binders and synthetic stone casting, as well as calculating the amount of carbon dioxide absorbed and stored by the slag during storage at the landfill.

Comparing the results obtained with similar approaches [37–39], it should be noted that deep learning algorithms are structurally different from traditional chemometric methods and have significantly more parameters [40]. Therefore, using deep learning algorithms to build efficient calibration models for determining the composition of slag can be challenging for both the developer and the end operator. The proposed approach provides diagnostic tools and rapid determination of granulated blast furnace slag composition with accuracy comparable to modern deep learning algorithms.

4. Conclusions

The EDX method was used to evaluate the structure and elemental composition of a series of granulated slag samples.

Interpretation of FTIR spectra of a series of samples of granulated blast furnace slag was carried out and the absorption bands that make the greatest contribution to their differences in composition were identified.

Multivariate regression methods (regression on principal components, projection to latent structures) and data of elemental composition results by EDX method were used to develop calibration models for determining elemental composition of granulated blast furnace slag. Using the developed PLS models, prediction of the elemental composition of a test sample was carried out.

The possibility of using a combination of infrared spectroscopy and multivariate analysis methods for rapid and nondestructive identification of the composition of granulated blast furnace slag has been demonstrated.

The approach proposed in our work is simple and has the potential to be used in automatic mode. The developed chemometric models allow quick and precise deter-

mination of slag composition, with minimal sample preparation and have potential for industrial application.

Subsequent research will focus on expanding the range of application of this method, namely for the identification of other metallurgical wastes and in mining and geological prospecting activities.

Author Contributions: Conceptualization, D.A.M., I.N.B. and N.V.K.; methodology, Y.T.P., B.B.K. and E.A.K.; software, D.A.M., E.A.K. and N.V.K.; validation, D.A.M., P.O.O., A.V.G. and Y.T.P.; formal analysis, Y.T.P. and N.V.K.; resources, B.B.K., E.A.K. and T.B.K.; data curation, B.B.K. and T.B.K.; writing—original draft preparation, D.A.M., N.V.K.; writing—review and editing, I.N.B., Y.T.P. and D.V.K.; visualization, B.B.K. and N.V.K.; supervision, I.N.B., P.O.O. and Y.T.P.; project administration, I.N.B. and D.V.K. All authors have read and agreed to the published version of the manuscript.

Funding: This research was funded by the Ministry of Science and Higher Education of the Russian Federation (NUST "MISIS" grant No K2-2020-009).

Acknowledgments: This research was partially financially supported by the Ministry of Science and Higher Education of the Russian Federation in the framework of Strategic Academic Leadership Program "Priority 2030", NUST "MISIS" grant No K2-2020-009.

Conflicts of Interest: The authors declare no conflict of interest.

References

1. Piatak, N.M.; Ettler, V. Introduction: Metallurgical Slags—Environmental Liability or Valuable Resource? In *Metallurgical Slags: Environmental Geochemistry and Resource Potential*; Piatak, N.M., Ettler, V., Eds.; The Royal Society of Chemistry: Cambridge, UK, 2021; pp. 1–13.
2. Gaskell, D.R. The Determination of Phase Diagrams for Slag Systems. In *Methods for Phase Diagram Determination*; Elsevier: Amsterdam, The Netherlands, 2007; pp. 442–458.
3. Mahasenan, N.; Smith, S.; Humphreys, K.; Kaya, Y. The cement industry and global climate change: Current and potential future cement industry CO_2 emissions. In Proceedings of the 6th International Conference on Greenhouse Gas Control Technologies, Kyoto, Japan, 1–4 October 2002; pp. 995–1000.
4. Bernal, S.A.; Gutierrez, R.M.; Provis, J.L. Engineering and durability properties of concrete based on alkali-activated granulated blast furnace slag/metakaolin blends. *Constr. Build. Mater.* **2012**, *33*, 99–108. [CrossRef]
5. Madavarapu, S.B.; Neithalath, N.; Rajan, S.; Marzke, R. FTIR Analysis of Alkali Activated Slag and Fly Ash Using Deconvolution Techniques. Master's Thesis, Arizona State University, Tempe, AZ, USA, 2014.
6. Brandaleze, E.; Benavidez, E.; Santini, L. Treatments and recycling of metallurgical slags. In *Recovery and Utilization of Metallurgical Solid Waste*; Zhang, Y., Ed.; IntechOpen: London, UK, 2018; Section 3; pp. 35–52.
7. Mohassab, Y.; Sohn, H.Y. Analysis of Slag Chemistry by FTIR-RAS and Raman Spectroscopy: Effect of Water Vapor Content in H_2-H_2O-CO-CO_2 Mixtures Relevant to a Novel Green Ironmaking Technology. *Steel Res. Int.* **2015**, *86*, 740–752. [CrossRef]
8. Goncharova, M. Application of slag from ferrous metal industry in asphalt concrete. In Proceedings of the International Conference "Modernisation and Researches in Transport System", Perm, Russia, 24 April 2014.
9. Kozhukhova, N.; Kadyshev, N.; Cherevatova, A.; Voitovich, E.; Lushin, K. Reasonability of application of slags from metallurgy industry in road construction. In *Advances in Intelligent Systems and Computing*; Murgul, V., Popovic, Z., Eds.; Springer: Berlin/Heidelberg, Germany, 2017; Volume 692, pp. 776–782.
10. Zhang, H.; Dong, J.; Wei, C. Material Properties of Cement Doped with Carbonated Steel Slag Through the Slurry Carbonation Process: Effect and Quantitative Model. *Metall. Mater. Trans. B* **2022**, *53*, 1681–1690. [CrossRef]
11. Gorokhovsky, A.; Escalante-Garcia, J.I.; Gorokhovsky, V.; Mescheryakov, D. Inorganic wastes in the manufacture of glass and glass-ceramics: Quartz-feldspar waste of ore refining, metallurgical slag, limestone dust, and phosphorus slurry. *J. Am. Ceram. Soc.* **2002**, *85*, 285–287. [CrossRef]
12. Neeladharan, C. Stabilization of soil using Fly ash with ground granulated blast furnace slag (GGBS) as binder. *Suraj Punj. J.* **2019**, *9*, 23.
13. Amulya, S.; Ravi Shankar, A.U.; Praveen, M. Stabilization of lithomargic clay using alkali activated fly ash and ground granulated blast furnace slag. *Int. J. Pavement Eng.* **2020**, *21*, 1114–1121. [CrossRef]
14. Sihag, P.; Suthar, M.; Mohanty, S. Estimation of UCS-FT of Dispersive Soil Stabilized with Fly Ash, Cement Clinker and GGBS by Artificial Intelligence. *Iran. J. Sci. Technol. Trans. Civ. Eng.* **2021**, *45*, 901–912. [CrossRef]
15. Ghaffoori, F.K.; Arbili, M.M. Effects of Fly Ash and Granulated Ground Blast Furnace Slag on Stabilization of Crude Oil Contamination Sandy Soil. *Polytech. J.* **2019**, *9*, 80–85. [CrossRef]
16. Miraki, H.; Shariatmadari, N.; Ghadir, P.; Jahandari, S.; Tao, Z.; Siddique, R. Clayey soil stabilization using alkali-activated volcanic ash and slag. *J. Rock Mech. Geotech. Eng.* **2021**, *14*, 576–591. [CrossRef]
17. Kumar, P.G.; Harika, S. Stabilization of expansive subgrade soil by using fly ash. *Mater. Today Proc.* **2020**, *45*, 6558–6562. [CrossRef]

18. Thomas, A.; Tripathi, R.K.; Yadu, L.K. A Laboratory Investigation of Soil Stabilization Using Enzyme and Alkali-Activated Ground Granulated Blast-Furnace Slag. *Arab. J. Sci. Eng.* **2018**, *43*, 5193–5202. [CrossRef]
19. Sharma, K.; Kumar, A. Utilization of industrial waste—Based geopolymers as a soil stabilizer—A review. *Innov. Infrastruct. Solut.* **2020**, *5*, 97. [CrossRef]
20. Phummiphan, I.; Horpibulsuk, S.; Rachan, R.; Arulrajah, A.; Shen, S.; Chindaprasirt, P. High calcium fly ash geopolymer stabilized lateritic soil and granulated blast furnace slag blends as a pavement base material. *J. Hazard. Mater.* **2017**, *341*, 257–267. [CrossRef] [PubMed]
21. Aziz, I.H. Behaviour changes of ground granulated blast furnace slag geopolymers at high temperature. *Adv. Cem. Res.* **2019**, *32*, 465–475. [CrossRef]
22. Stumpe, B.; Engel, T.; Steinweg, B.; Marschner, B. Application of PCA and SIMCA statistical analysis of FT-IR spectra for the classification and identification of different slag types with environmental origin. *Environ. Sci. Technol.* **2012**, *46*, 3964–3972.
23. Rovnaník, P.; Bayer, P.; Rovnaníková, P. Characterization of alkali activated slag paste after exposure to high temperatures. *Constr. Build. Mater.* **2013**, *47*, 1479–1487. [CrossRef]
24. Lodeiro, I.G.; Macphee, D.E.; Palomo, A.; Fernández-Jiménez, A. Effect of alkalis on fresh C–S–H gels. FTIR analysis. *Cem. Concr. Res.* **2009**, *39*, 147–153. [CrossRef]
25. Puertas, F.; Fernández-Jiménez, A. Mineralogical and microstructural characterisation of alkali-activated fly ash/slag pastes. *Cem. Concr. Compos.* **2003**, *25*, 287–292. [CrossRef]
26. Puertas, F.; Fernández-Jiménez, A.; Blanco-Varela, M.T. Pore solution in alkali-activated slag cement pastes. Relation to the composition and structure of calcium silicate hydrate. *Cem. Concr. Res.* **2004**, *34*, 139–148. [CrossRef]
27. Sowmya, T.; Sankaranarayanan, S.R. Spectroscopic analysis of slags-preliminary observation. In Proceedings of the VII International Conference on Molten Slags, Fluxes and Salts, Cape Town, South Africa, 25–28 January 2004.
28. Bitay, E.; Kacsó, I.; Tănăselia, C.; Toloman, D.; Borodi, G.; Pánczél, S.P.; Veress, E. Spectroscopic Characterization of Iron Slags from the Archaeological Sites of Brâncoveneşti, Călugăreni and Vătava Located on the Mureş County (Romania) Sector of the Roman Limes. *Appl. Sci.* **2020**, *10*, 5373. [CrossRef]
29. Korovkin, M.V. *Infrared Spectroscopy of Carbonate Minerals*; National Research Tomsk Polytechnic University: Tomsk, Russia, 2012; pp. 40–80.
30. Platov, Y.T.; Platova, R.A.; Molodkina, P.G. Using Decomposition of IR Spectra to Analyze Structural-Phase Transformations of Kaolinite. *J. Appl. Spectrosc.* **2021**, *87*, 1029–1036. [CrossRef]
31. Madsen, I.C.; Scarlett, N.V.; Cranswick, L.M.; Lwin, T. Outcomes of the International Union of Crystallography Commission on powder diffraction round robin on quantitative phase analysis: Samples 1a to 1h. *J. Appl. Crystallogr.* **2001**, *34*, 409–426. [CrossRef]
32. Taganova, A.A.; Boychenko, E.A.; Kiselev, N.V.; Khaidarov, B.B.; Kolesnikov, E.A.; Yudin, A.G.; Burmistrov, I.N. Synthesis and Study of the Composition of Hollow Microspheres of NiO and NiO/Ni Composition for Thermoelectrochemical Energy Converters of Low-Potential Temperature Gradients of Thermal Units into Electricity. *Refract. Ind. Ceram.* **2021**, *61*, 715–719. [CrossRef]
33. Mercado-Borrayo, B.M.; Schouwenaars, R.; Litter, M.I.; Montoya-Bautista, C.V.; Ramírez-Zamora, R.M. *Metallurgical Slag as an Efficient and Economical Adsorbent of Arsenic in Water Reclamation and Sustainability*; Elsevier: Amsterdam, The Netherlands, 2014; pp. 95–114.
34. Čabanová, K.; Vlček, J.; Seidlerová, J.; Matějka, V.; Peikertová, P.; Martausová, I.; Kukutschová, J. Chemical and phase composition of metallurgical slags and their effects on freshwater green algae. *Mater. Today Proc.* **2018**, *5*, S2–S10. [CrossRef]
35. Ptáček, P.; Šoukal, F.; Opravil, T.; Nosková, M.; Havlica, J.; Brandštetr, J. Mid-infrared spectroscopic study of crystallization of cubic spinel phase from metakaolin. *J. Solid State Chem.* **2011**, *184*, 2661–2667. [CrossRef]
36. Zhu, F.; Wu, X.; Zhou, M.; Sabri, M.M.; Huang, J. Intelligent design of building materials: Development of an ai-based method for cement-slag concrete design. *Materials* **2022**, *15*, 3833. [CrossRef]
37. Shah, S.A.R.; Azab, M.; Seif ElDin, H.M.; Barakat, O.; Anwar, M.K.; Bashir, Y. Predicting Compressive Strength of Blast Furnace Slag and Fly Ash Based Sustainable Concrete Using Machine Learning Techniques: An Application of Advanced Decision-Making Approaches. *Buildings* **2022**, *12*, 914. [CrossRef]
38. Han, I.J.; Yuan, T.F.; Lee, J.Y.; Yoon, Y.S.; Kim, J.H. Learned Prediction of Compressive Strength of GGBFS Concrete Using Hybrid Artificial Neural Network Models. *Materials* **2019**, *12*, 3708. [CrossRef] [PubMed]
39. Dao, D.V.; Ly, H.B.; Trinh, S.H.; Le, T.-T.; Pham, B.T. Artificial intelligence approaches for prediction of compressive strength of geopolymer concrete. *Materials* **2019**, *12*, 983. [CrossRef]
40. Hu, X.; Chu, L.; Pei, J.; Liu, W.; Bian, J. Model complexity of deep learning: A survey. *Knowl. Inf. Syst.* **2021**, *63*, 2585–2619. [CrossRef]